

RSC Advances



This is an *Accepted Manuscript*, which has been through the Royal Society of Chemistry peer review process and has been accepted for publication.

Accepted Manuscripts are published online shortly after acceptance, before technical editing, formatting and proof reading. Using this free service, authors can make their results available to the community, in citable form, before we publish the edited article. This *Accepted Manuscript* will be replaced by the edited, formatted and paginated article as soon as this is available.

You can find more information about *Accepted Manuscripts* in the [Information for Authors](#).

Please note that technical editing may introduce minor changes to the text and/or graphics, which may alter content. The journal's standard [Terms & Conditions](#) and the [Ethical guidelines](#) still apply. In no event shall the Royal Society of Chemistry be held responsible for any errors or omissions in this *Accepted Manuscript* or any consequences arising from the use of any information it contains.

Cite this: DOI: 10.1039/c0xx00000x

www.rsc.org/xxxxxx

ARTICLE TYPE

Novel PA-doped polybenzimidazole membranes with high doping level, high proton conductivity and high stability for HT-PEMFCs

Xiaobai Li,^a Hongwei Ma,^a Hailong Wang,^a Shitong Zhang,^a Zhenhua Jiang,^a Baijun Liu^{*a} and Michael D. Guiver^b

Received (in XXX, XXX) XthXXXXXXXXXX 20XX, Accepted Xth XXXXXXXXXXXX 20XX
DOI: 10.1039/b000000x

A novel high temperature proton exchange membrane (HT-PEM) with high phosphoric acid (PA) doping level of 24.6, high proton conductivity of $0.217 \text{ S}\cdot\text{cm}^{-1}$ at $200 \text{ }^\circ\text{C}$, as well as excellent mechanical-dimensional stability was prepared based on a structure-designed polybenzimidazole (PBI).

Over the past several decades, proton exchange membrane fuel cells (PEMFCs) have spurred tremendous interest due to their excellent promise as clean and efficient electrochemical conversion devices.¹ Typical PEMFCs operating at temperatures below $100 \text{ }^\circ\text{C}$ have some drawbacks caused by the water-based proton-conduction mechanism. In contrast, high temperature proton exchange membrane fuel cells (HT-PEMFCs) operating at $100\text{--}200 \text{ }^\circ\text{C}$ offers several benefits, for instance, reduced CO poisoning of platinum electrocatalyst, fast electrode kinetics, simplified water/thermal management and increased resistance to fuel impurities.² DuPont's Nafion, which has been successfully applied in industry, exhibits high proton conductivity ($10^{-1} \text{ S}\cdot\text{cm}^{-1}$) at lower temperatures ($\leq 80 \text{ }^\circ\text{C}$) under high relative humidity (100 % RH). However, it has low efficiency at operating temperatures over $100 \text{ }^\circ\text{C}$. Thus, the development of proton exchange membranes (PEMs) operating at $100\text{--}200 \text{ }^\circ\text{C}$ is one of the most important topics in the field and a great deal of effort has been invested by both industry and academia.³

In the 1990s, researchers at Case Western Reserve University first used phosphoric acid (PA)-doped poly(2,2'-(1,3-phenylene)-5,5'-bibenzimidazole) (*m*-PBI) as an electrolyte membrane for HT-PEMFCs.⁴ In this PA-imidazole system, protons transfer from one site to another through the formation and breaking of hydrogen bonds, and the main proton-conduction mechanism changes from vehicle-type to Grotthuss-type.⁵ As promising membranes for HT-PEMs, PA-PBIs possess many attractive properties and thus have received a great deal of contemporary interest. Until now, however, relatively few PBI structures, such as *m*-PBI and poly(2,5-benzimidazole) (ABPBI)^{2(a)}, have been studied for PA-imidazole systems. Based on *m*-PBI or ABPBI, some strategies including grafting,⁶ crosslinking,⁷ inorganic doping,⁸ polymer blending,⁹ and sol-gel method¹⁰ have been adopted to improve the performance of the PEMs. For example, Lee and Choi^{7(c)} prepared a PA-doped cross-linked benzoxazine-benzimidazole membrane and achieved a proton conductivity of $0.12 \text{ S}\cdot\text{cm}^{-1}$ at $150 \text{ }^\circ\text{C}$ under anhydrous conditions. Unfortunately, after immersed the membrane in PA solution at $160 \text{ }^\circ\text{C}$ for 5 h,

the membrane partially dissolved and lost its shape. He and Li^{6(a)} reported a series of PA-doped benzimidazole-grafted-polybenzimidazole membranes, which could have the highest PA doping level (ADL) of 22.5 and exhibited the highest conductivity of $0.295 \text{ S}\cdot\text{cm}^{-1}$ at $180 \text{ }^\circ\text{C}$. However, its tensile strength was only 2 MPa at room temperature, which was too weak to be handled during the MEA preparation. In addition, the area and volume swelling were as high as 157 % and 360 %, respectively. As one can see from the above representative PA-PBIs membranes, high acid doping levels (ADLs) usually led to high conductivity but also accompanied by sacrificing too much mechanical and dimensional stability.¹¹ No markedly successful approaches have thus far improved the overall desired balance of properties for HT-PEMs based on traditional PBIs. This motivated us to explore PBIs with novel structures, in order to expand the scope of study with the aim of improving the overall balance of properties of HT-PEMs.

For the purpose of achieving PA-PBI membranes with high conductivity as well as high mechanical and dimensional stability, a novel PBI was investigated. We hypothesize that the preferred polymer membrane should have a more open "sponge-like" structure which can both hold considerable liquid and maintain original shape at a high level of liquid absorption. For the corresponding molecular design, the desired PBI should have two main features to construct a "sponge-like" microstructure of membrane that can meet the performance requirements. That is, the ideal microstructure should provide "free volume" to hold excess acid molecules and a framework to maintain mechanical strength.

Accordingly, we introduced flexible ether linkages ($-\text{O}-$) and side groups (phenyl) onto the PBI backbone. The selected PBI in this communication is denoted as Ph-PBI. The introduction of ether linkages may facilitate the entanglement between molecular chains thus forming intertwined polymer networks. Also, the interactions of imidazole groups will be helpful to form a stable framework. The side groups with large steric hindrance will disrupt the close polymer chain packing and reduce molecular chain packing density, to increase the "free volume" in the supposed "sponge-like" structure. Furthermore, to make a direct comparison, poly[2,2'-(*p*-oxydiphenylene)-5,5'-bibenzimidazole] (OPBI)¹² having linear molecular structure was prepared by the same polymerization method. The PA-PBI samples were obtained by immersing the membranes (OPBI and Ph-PBI) in a dish with

85 wt% PA solution at 160 °C for 3, 12, 36, 72, 108 h, respectively. The samples are named as O-3, O-12, and Ph-3, Ph-

12, Ph-36, Ph-72, Ph-108, respectively.

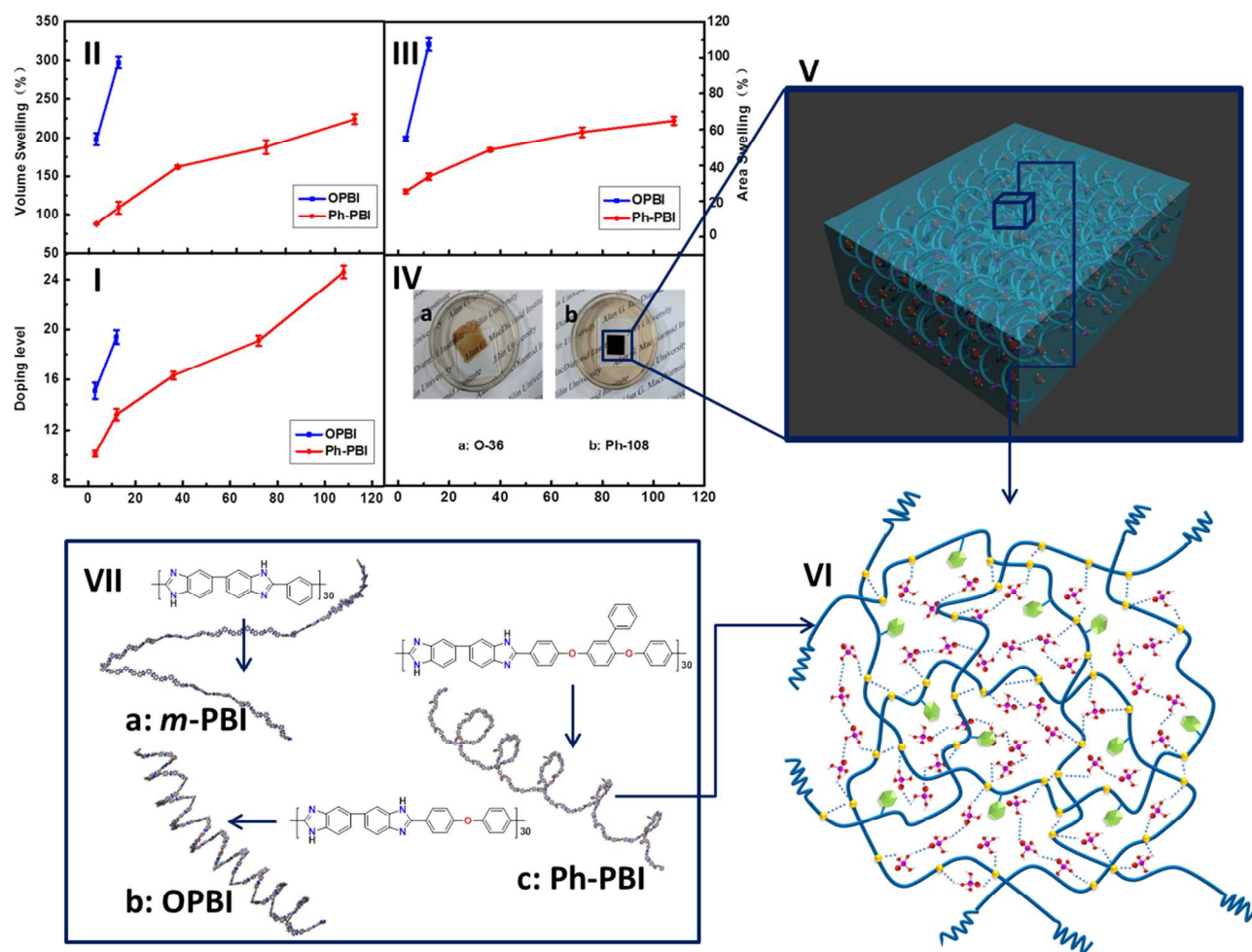


Fig. 1 (I-III) Doping levels, volume swelling ratios and area swelling ratios of membranes as a function of doping time; (IV) Photos of O-36 and Ph-108; (V) The hypothetical “sponge-like” packing for PA-Ph-PBI; (VI) The loose molecular structure of PA-Ph-PBI; (VII) The results of the molecular simulation of *m*-PBI(a), OPBI(b) and Ph-PBI(c).

Table S2 shows the ADLs and corresponding area, thickness and volume swellings of PA-PBI membranes. The ADLs, volume and area swellings increased with increasing doping time for all samples, as shown in Fig. 1 I-III. It could be observed that OPBI membranes had a faster PA doping rate at the initial stage compared to Ph-PBI membranes. At the same doping time, OPBI membranes exhibited ADLs about 1.5 times higher than those of Ph-PBI ones. However, it was surprising to find that the volume and area swelling ratios of OPBI membranes were about 2-3 times higher than those of Ph-PBI membranes. As a result, the swelling of the OPBI membrane was too large to be measured and lost the capability to maintain the original regular shape after 36 h treatment (Fig. 1 IV), and the 72 and 108 h treated OPBI membranes could not be tested. However, Ph-PBI exhibited quite different absorption process and results. The 72 h treated Ph-PBI (Ph-72) reached the ADL of 19.1, which was similar to that of 12 h treated OPBI (O-12). It is worth noting that after absorption for the long time of 108 h, Ph-108 achieved extremely high ADLs of 24.6. However, it had acceptably low dimensional change (Fig. 1 IV). In contrast, O-12 had ADL of 19.4, which was lower than

the levels of Ph-108. However, O-12 exhibited the volume swelling about 1.4 times and the area swelling about 1.7 times higher than those of Ph-108. Given the importance of the dimensional stability of PA-doping membranes, a wider comparison with other reported work has been made in Table S2. At the similar ADLs, the membranes reported by others showed much higher volume swelling, and some even possessed the volume swelling about 2-3 times higher than our Ph-PBI.¹³ To further explain the excellent dimensional stability of these novel membranes from the perspective of molecular structure, the molecular simulation of *m*-PBI, OPBI and Ph-PBI of 30 repeating units was made using the UFF method (Universal Force Field) on Gaussian 09 Version D01, and the results are shown in Fig. 1 VII. Ph-PBI had the loose helix molecular chains, which was prone to pack and form the “sponge-like” structure (Fig. 1 V and VI). These were highly related with chemical structure of Ph-PBI with two flexible ether linkages and one rigid biphenyl moiety per repeating unit, which would partially disrupt close chain packing caused by H-bonding interactions of the imidazole groups. This is proved by its relatively low density of 1.25 g·cm⁻³, large FFV

(0.138) and large d_{sp} (4.91 Å) (Table S1). In comparison, conventional *m*-PBI with more rigid molecular chains had a trend to form a tight structure, and OPBI with more regular and less flexible molecular chains may form a denser structure with fewer tangles. The enlarged images of molecular simulation can be seen in Fig. S4. Another interesting observation is that the Ph-PBI membranes display anisotropic swelling behaviour, and the area swelling ratios were much lower than that of the thickness (Table S2). This preferred behaviour may minimize the structural breakage of MEAs and, thereby, enhance fuel cell durability and performance.¹⁴ in Fig. S4. Another interesting observation is that the Ph-PBI membranes display anisotropic swelling behaviour, and the area swelling ratios were much lower than that of the thickness (Table S2). This preferred behaviour may minimize the structural breakage of MEAs and, thereby, enhance fuel cell durability and performance.¹⁴

Good mechanical properties are important for the membranes to withstand high temperatures and pressure when they are utilized in HT-PEMFCs. Ph-PBI membranes had high tensile strengths of 106.7 MPa. Polymer chain intermolecular forces are reduced by the plasticizing effect of the doping acid, resulting in a reduction in tensile strength with increasing amounts of ADLs.^{6(a)} In this study, Ph-PBI membranes showed higher tensile stress in comparison with other reported PA-PBI membranes at similar ADLs (Table S2).¹³ After 3 h treatment in PA, the tensile strengths of Ph-3 was 22.3 MPa. In contrast, the tensile strength of OPBI series sharply decreased with doping time, and O-3 only had a tensile strength of 2.8 MPa (Table S2). That is to say, Ph-PBI membranes treated with PA have more excellent mechanical stability than O-PBI membranes.

Proton conductivity is one of the most important performance parameters for PEMs to be effectively applied in fuel cells. As expected, the proton conductivities under anhydrous conditions

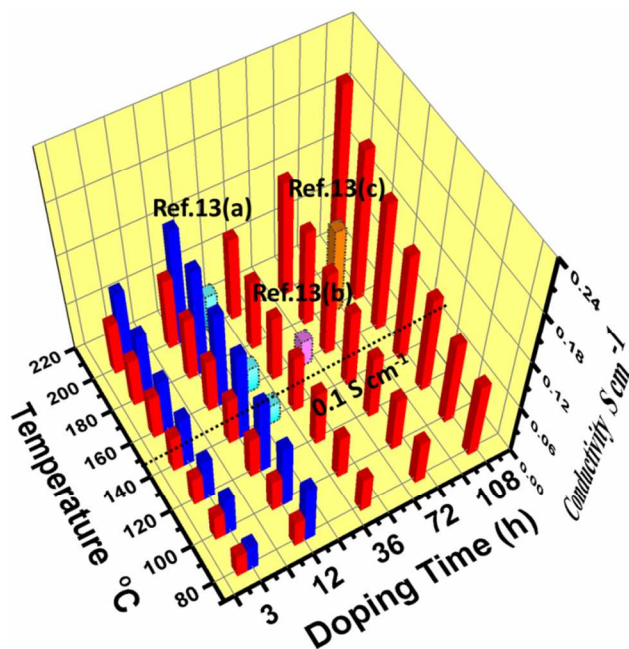


Fig. 2 Conductivities of the OPBI (blue) and Ph-PBI (red) membranes. The dotted columns (blue, purple and orange) were from the reported representative data¹³ as references.

increased for all membranes with increasing doping time and test temperature (Table S2 and Fig. 2). Although OPBI membranes had high conductivities (e.g. O-12 0.142 S·cm⁻¹ at 200 °C) owing to their high ADLs within short doping times, their tensile strengths were insufficient. On the contrary, Ph-108 membrane had sufficiently high ADL and accordingly high conductivity, which were much higher than those of O-12. In particular, Ph-108 membrane achieved high conductivity of 0.217 S·cm⁻¹ at 200 °C, and exhibited good dimensional stability and strength under these conditions. Excitingly, the conductivity of Ph-108 is considerably higher than other reported results on the analogues,¹³ as shown in Fig. 2. It should be mentioned that the U.S. Department of Energy has a currently established guideline that the target conductivity at 120 °C should reach 0.1 S·cm⁻¹ for PEMs in automotive applications.¹⁵ In our study, the conductivities of Ph-108 was 0.119 S·cm⁻¹ at 120 °C. Hence, the PBI material is possible candidate for HT-PEMs.

Membranes with sufficient mechanical properties (O-3 and Ph-72) were fabricated into MEAs and tested in fuel cells at 160 °C and atmospheric pressure. The polarization curves and power density curves are shown in Fig. 3. At a current density of 0.2 A cm⁻², Ph-72 and O-3 membranes show voltages of 0.59 V and 0.49 V, respectively. The maximum power densities of Ph-72 and O-3 membranes are 279 and 144 mW cm⁻², respectively. As seen from these results, Ph-72 membrane exhibits much better fuel cell performance than that of O-3 membrane. This much improved performance demonstrates that PA-doped Ph-PBI membranes have the feasibility of being used in HT-PEMs.

In summary, the proton conductivity of HT-PEMs is usually increased by raising ADLs, but at the expense of sacrificing the mechanical and dimensional stability. In the present work, we prepared novel HT-PEMs which simultaneously have high acid doping levels, high proton conductivity, high stability and excellent fuel cell performances. We suggest the excellent overall performance is related to a more open “sponge-like” membrane structure, which is supported by the molecular modelling, the low tested density, large FFV and large d_{sp} results of membranes. This work provides a new insight for the structural design of PBIs for HT-PEMs.

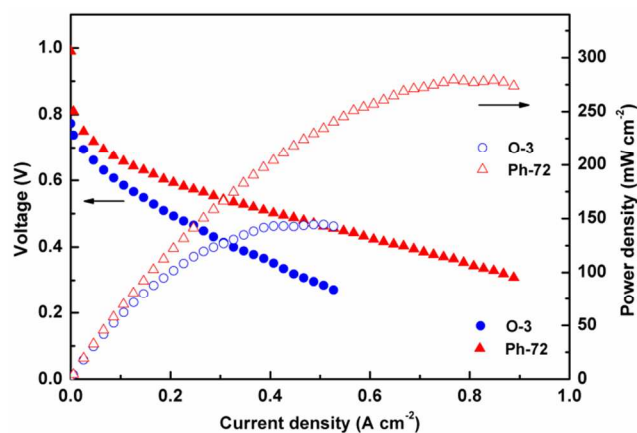


Fig.3 Fuel cell performance of Ph-72 and O-3 membranes at 160 °C: polarization curves (filled symbols) and power density curves (open symbols).

Financial support for this project was provided by the National

Natural Science Foundation (No.: 50973040), the Science and Technology Development Plan of Jilin Province (No.: 20130521003JH and 20140204016GX), the Key Technology Research and Development Program of Changchun City (No.: 13KG36), and Industrial Technology Research and Development Funds of Jilin Province, China (No.: 2011004-1).

Notes and references

^a Alan G. MacDiarmid Institute, College of Chemistry, Jilin University, 2699 Qianjin Street, Changchun 130012, P. R. China. Fax: 86-431-85168022; Tel: 0431-85168022; E-mail: liubj@jlu.edu.cn

^b State Key Laboratory of Engines, School of Mechanical Engineering, and Collaborative Innovation Center of Chemical Science and Engineering (Tianjin), Tianjin University, Tianjin 300072, China. Tel/Fax: 86-22-27404479; E-mail: michael.guiver@outlook.com

† Electronic Supplementary Information (ESI) available: [details of any supplementary information available should be included here]. See DOI: 10.1039/b000000x/

‡ Footnotes should appear here. These might include comments relevant to but not central to the matter under discussion, limited experimental and spectral data, and crystallographic data.

- (a) B. Campagne, G. David, B. Améduri, D. J. Jones, J. Rozière and I. Roche, *Macromolecules*, 2013, **46**, 3046-3057; (b) J. A. Mader and B. C. Benicewicz, *Macromolecules*, 2010, **43**, 6706-6715; (c) H. Tang, M. Pan, S. Lu, J. Lu and S. P. Jiang, *Chem. Commun.*, 2010, **46**, 4351-4353; (d) M. L. Einsla, Y. S. Kim, M. Hawley, H. S. Lee, J. E. McGrath, B. Liu, M. D. Guiver and B. S. Pivovar, *Chem. Mater.*, 2008, **20**, 5636-5642; (e) D. Mecerreyes, H. Grande, O. Miguel, E. Ochoteco, R. Marcilla and I. Cantero, *Chem. Mater.*, 2004, **16**, 604-607; (f) Z. Liu, X. Li, K. Shen, P. Feng, Y. Zhang, X. Xu, W. Hu, Z. Jiang, B. Liu and M. D. Guiver, *J. Mater. Chem. A*, 2013, **1**, 6481-6488.
- (a) J. A. Asensio, E. M. Sánchez and P. Gómez-Romero, *Chem. Soc. Rev.*, 2010, **39**, 3210-3239; (b) S. Bose, T. Kuila, T. X. H. Nguyen, N. H. Kim, K. Lau and J. H. Lee, *Prog. Polym. Sci.*, 2011, **36**, 813-843; (c) Suryani, Y. Chang, J. Lai and Y. Liu, *J. Membr. Sci.*, 2012, **403-404**, 1-7; (d) C. B. Shogbon, J. L. Brousseau, H. Zhang, B. C. Benicewicz and Y. A. Akpalu, *Macromolecules*, 2006, **39**, 9409-9418; (e) P. Jannasch, *Curr. Opin. Colloid Interface Sci.*, 2003, **8**, 96-102; (f) W. Han and K. L. Yeung, *Chem. Commun.*, 2011, **47**, 8085-8087. (g) J. Weber, K. D. Kreuer, J. Maier and A. Thomas, *Adv. Mater.*, 2008, **20**, 2595-2598.
- (a) M. Geormezi, V. Deimede, N. Gourdoupi, N. Triantafyllopoulos, S. Neophytides and J. K. Kallitsis, *Macromolecules*, 2008, **41**, 9051-9056; (b) J. Zeng, B. He, K. Lamb, R. D. Marco, P. K. Shenc and S. P. Jiang, *Chem. Commun.*, 2013, **49**, 4655-4657.
- J. S. Wainright, J. T. Wang, D. Weng, R. F. Savinell and M. J. Litt, *J. Electrochem. Soc.*, 1995, **142**, 121-123.
- (a) Z. Zuo, Y. Fu and A. Manthiram, *Polymers*, 2012, **4**, 1627-1644; (b) C. Nagamani, U. Viswanathan, C. Versek, M. T. Tuominen, S. M. Auerbach and S. Thayumanavan, *Chem. Commun.*, 2011, **47**, 6638-6640; (c) D. Basak, C. Versek, D. T. Toscano, S. Christensen, M. T. Tuominen and D. Venkataraman, *Chem. Commun.*, 2012, **48**, 5922-5924.
- (a) J. Yang, D. Aili, Q. Li, Y. Xu, P. Liu, Q. Che, J. O. Jensen, N. J. Bjerrum and R. He, *Polym. Chem.*, 2013, **4**, 4768-4775; (b) T. H. Tang, P. H. Su, Y. C. Liu and T. L. Yu, *Int. J. Hydrogen Energy*, 2014, **39**, 11145-11156.
- (a) D. Aili, Q. Li, E. Christensen, J. O. Jensen and N. J. Bjerrum, *Polym Int.*, 2011, **60**, 1201-1207; (b) M. Han, G. Zhang, Z. Liu, S. Wang, M. Li, J. Zhu, H. Li, Y. Zhang, C. M. Lew and H. Na, *J. Mater. Chem.*, 2011, **21**, 2187-2193; (c) S. K. Kim, S. W. Choi, W. S. Jeon, J. O. Park, T. Ko, H. Chang and J. C. Lee, *Macromolecules*, 2012, **45**, 1438-1446.
- (a) R. Kannan, H. N. Kagalwala, H. D. Chaudhari, U. K. Kharul, S. Kurungot and V. K. Pillai, *J. Mater. Chem.*, 2011, **21**, 7223-7231; (b) D. Plackett, A. Siu, Q. Li, C. Pan, J. O. Jensen, S. F. Nielsen, A. A. Permyakova and N. J. Bjerrum, *J. Membr. Sci.*, 2011, **383**, 78-

87; (c) C. Xu, Y. Cao, R. Kumar, X. Wu, X. Wang and K. Scott, *J. Mater. Chem.*, 2011, **21**, 11359-11364.

- (a) S. Singha and T. Jana, *Polymer*, 2014, **55**, 594-601; (b) Q. F. Li, H. C. Rudbeck, A. Chromik, J. O. Jensen, C. Pan, T. Steenberg, M. Calverley, N. J. Bjerrum and J. Kerres, *J. Membr. Sci.*, 2010, **347**, 260-270.
- (a) L. Xiao, H. Zhang, E. Scanlon, L. S. Ramanathan, E. W. Choe, D. Rogers, T. Apple and B. C. Benicewicz, *Chem. Mater.*, 2005, **17**, 5328-5333; (b) L. Xiao, H. Zhang, T. Jana, E. Scanlon, R. Chen, E. W. Choe, L. S. Ramanathan, S. Yu and B. C. Benicewicz, *Fuel Cells*, 2005, **5**, 287-295.
- Q. Li, C. Pan, J. O. Jensen, P. Noye and N. J. Bjerrum, *Chem. Mater.*, 2007, **19**, 350-352.
- S. Subianto, *Polym Int.*, 2014, **63**, 1134-1144.
- (a) S. Wang, C. Zhao, W. Ma, G. Zhang, Z. Liu, J. Ni, M. Li, N. Zhang, H. Na, *J. Membr. Sci.*, 2012, **411-412**, 54-63; (b) J. Yang, Q. Li, L. N. Cleemann, C. Xu, J. O. Jensen, C. Pan, N. J. Bjerrum and R. He, *J. Mater. Chem.*, 2012, **22**, 11185-11195; (c) J. Yang, Y. Xu, L. Zhou, Q. Che, R. He, Q. Li, *J. Membr. Sci.*, 2013, **446**, 318-325.
- C. H. Lee, S. Y. Lee, Y. M. Lee, S. Y. Lee, J. W. Rhim, O. Lane and J. E. McGrath, *ACS Appl. Mater. Interfaces*, 2009, **1** (5) 1113-1121.
- M. A. Hickner, H. Ghassemi, Y. S. Kim, B. R. Einsla and J. E. McGrath, *Chem. Rev.*, 2004, **104**, 4587-4611.